https://doi.org/10.5194/egusphere-2026-731
Preprint. Discussion started: 19 February 2026

Riverine Organic Matter Dynamics in the Headwaters of the China's Yellow River under Climate Change

Xiaoxiao Wang [1,2], Jie Wang [1], Tianqing Ren [1], Jun Zhou [3]

[1] School of Geographical Sciences, China West Normal University, Nanchong 637009, China

[2] Sichuan Provincial Engineering Research Center of Monitoring and Control for Soil Erosion in Dry Valleys, China West Normal University, Nanchong 637009, China

[3] Institute of Mountain Hazards and Environment, Chinese Academy of Sciences, Chengdu 610213, China

Correspondence to: Xiaoxiao Wang (wxx1989@cwnu.edu.cn)

Xiaoxiao Wang and Jie Wang contributed equally to this work.

https://doi.org/10.5194/egusphere-2026-731
Preprint. Discussion started: 19 February 2026

Abstract: Alpine headwater streams play a crucial role in the global carbon cycle and are particularly sensitive to climate change. Riverine organic matter (ROM) mediates the transport and transformation of terrestrial carbon across aquatic systems. However, the response of ROM in headwater streams on the Qinghai–Tibetan Plateau (QTP) to climate change remains poorly understood due to scarce in situ measurements. In this study, we used machine learning models combining satellite data and geographical variables to reconstruct historical variations in Chemical Oxygen Demand (COD, a proxy for ROM) along the Yellow River's Headstream (YRHS), and to predict future changes under typical Shared Socioeconomic Pathways. The results indicate that COD levels in the midstream region of the YRHS, characterized by greater precipitation, higher soil organic matter, and denser vegetation, were relatively high (2.73 ± 1.63 mg L^{-1}) and exhibited an increasing trend (+0.44 mg L^{-1}) over the past decade. Driven primarily by increasing precipitation and temperature, COD levels are projected to rise in upstream and downstream areas but decline at midstream sites under SSP126, SSP245, and SSP585 by the 2100s. The annual export of COD from the midstream of the YRHS is expected to increase from 62.5 Gg to 81.6 Gg by 2100s due to projected increase in COD concentrations and discharge. Our findings identify the midstream region of the YRHS as a critical and climate-sensitive region for organic matter dynamics. Nevertheless, substantial uncertainties remain in the future ROM changes owing to the complex interactions among precipitation, warming, and their combined effects on carbon cycles in alpine catchments. Therefore, further research is required to improve our understanding of catchment-scale carbon dynamics on the QTP in the context of climate change.

Key words: Alpine River; Carbon cycle; Climate change; Remote sensing; Machine learning

https://doi.org/10.5194/egusphere-2026-731
Preprint. Discussion started: 19 February 2026

1 Introduction

Alpine regions represent some of the most vulnerable ecosystems to climate change, experiencing temperature increases nearly twice the global average (Aryal and Pokhrel, 2025; Kotlarski et al., 2023). Although these high-altitude environments cover only a small fraction of the Earth's surface, they provide essential ecosystem services, including freshwater supply, carbon storage, and biodiversity support (Aryal and Pokhrel, 2025; Chen et al., 2022; Hotaling et al., 2017). Among them, the Qinghai–Tibetan Plateau (QTP), often referred to as the "Third Pole", is the highest and one of the most climate-sensitive regions on Earth (Chen et al., 2022; Wang et al., 2023). In recent decades, the accelerated warming has triggered widespread environmental changes on the QTP, which are expected to significantly alter the sources, forms, and fluxes of carbon exports associated with permafrost degradation (Chen et al., 2022; Hong et al., 2025; Xu et al., 2024). Studies have shown that parts of the QTP have already shifted from carbon sinks to carbon sources and lateral transport of carbon has increased the riverine carbon fluxes on the QTP (L. Li et al., 2025). Riverine organic matter (ROM) plays a pivotal role in the biogeochemical cycles of carbon (Beusen et al., 2022; Giri, 2021; Hu et al., 2020; Regnier et al., 2022) and increase in ROM will pose threats to the water quality of rives on the QTP. Despite growing concern regarding the ROM and its ecological consequences, our understanding of ROM dynamics across the QTP remains limited. Therefore, there is an urgent need for high spatial resolution and long-term observations of ROM dynamics and their exports on the QTP.

Headwater streams account for approximately 61% of total riverine ROM efflux despite representing only 34–38% of total stream surface area (Ran et al., 2021). Over recent decades, climate change has substantially influenced the ROM dynamics of headstreams on the QTP (Yao

https://doi.org/10.5194/egusphere-2026-731
Preprint. Discussion started: 19 February 2026

et al., 2022). Long-term records show that the annual streamflow of headstreams in this region has generally increased over the past six decades (1962–2019) (Z. Zhang et al., 2024). Warming and wetting trends have contributed to higher ROM in the headwaters (Xu et al., 2024). Furthermore, climate-induced changes have intensified sediment erosion and enhanced associated ROM transport processes across the QTP (J. Li et al., 2023; Li et al., 2024; J. Li et al., 2025; Zhao et al., 2023). Nevertheless, fewer than 30% of headstreams across the QTP are consistently monitored (Li et al., 2024), leaving the responses of ROM dynamics in headwaters to climate change poorly constrained.

The limited understanding of ROM dynamics in alpine headwaters is largely due to the scarcity of long-term, continuous in-situ measurements, where data collection remains logistically challenging. In recent years, advances in remote sensing and machine learning have provided powerful alternatives for addressing these limitations, offering new opportunities to predict water quality and infer nutrient-related parameters across extensive spatial and temporal scales (Adegun et al., 2023; Zeng et al., 2023; Zhi et al., 2024). Satellite-derived indices such as reflectance ratios, the Normalized Difference Chlorophyll Index (NDCI), the Suspended Sediment Index (SSI), etc., have been increasingly employed to assess riverine organic matter, particularly when integrated with machine learning algorithms (Deng et al., 2024; Liu et al., 2021; Yan et al., 2025a). Consequently, integrating remote sensing data with in-situ measurements and machine learning holds significant potential for improving our understanding of ROM in headwaters and their responses to ongoing climate changing.

The headstreams of the Yellow River, located on the eastern QTP, constitute a crucial component of QTP's water resources and carbon cycling systems and have undergone substantial

https://doi.org/10.5194/egusphere-2026-731
Preprint. Discussion started: 19 February 2026

environmental changes in recent decades (Wen et al., 2024). Current study indicated that approximately 35% of the Yellow River's source region serves as a net carbon source, and the lateral transport of carbon accounts for 31% of net ecosystem production in the Yellow River's source region (L. Li et al., 2025). Although numerous studies have been carried out across the broader Yellow River Basin, they have not focused on the historical and future dynamics of ROM in the source region of the Yellow River (Deng et al., 2025; Lan et al., 2025), which is largely attributable to limited monitoring network coverage in this region. Therefore, given the critical role of the Yellow River headwaters in carbon cycling and downstream water quality and its sensitivity to climate change, there is an urgent need to investigate the dynamics of riverine organic matter in the headwaters of the Yellowing River under climate change.

According to previous studies, ROM is commonly estimated using Chemical Oxygen Demand (COD) as a proxy, which reflects the amount of oxygen required to oxidize organic carbon in river water (Liu et al., 2023; Wang et al., 2026). Accordingly, we focus on the source region of the Yellow River to develop COD predictive models by combining in situ water quality observations with satellite reflectance data and to assess future changes under the SSP126, SSP245, and SSP585 scenarios. The objectives are to: (1) quantify the decadal variability of COD in the headstreams of the Yellow River and identify its driving factors; (2) predict future changes in COD under projected climate change scenarios; and (3) estimate COD exports and assess their potential impacts on downstream ecosystems. This study aims to provide a comprehensive and scalable understanding of how climate change is reshaping riverine organic matter dynamics within one of the world's most critical headwater regions.

2 Methods and materials

https://doi.org/10.5194/egusphere-2026-731
Preprint. Discussion started: 19 February 2026

2.1 Study area

The source region of the Yellow River is situated in the eastern QTP (Fig. 1a), covering approximately 195,000 km², with elevations ranging from 2650 m to 6250 m. The mean annual temperature in this area ranges between −3.5 and 7.5 °C. The annual average precipitation in this area ranges from 420 to 705 mm, with the highest values occurring in the midstream region (Yang et al., 2023). The dominant land cover consists of alpine meadows and alpine steppes (Fig. S1). The area covers extensive permafrost and seasonally frozen ground, together covering more than 85% of the region (Z. Li et al., 2025; M. Yang et al., 2025). Under the combined influence of climate warming and anthropogenic disturbances, permafrost in the upper reaches of the Yellow River source region has shown a significant trend of degradation in recent decades (Yang et al., 2023). The headwater region of the Yellow River contains a dense network of tributaries and contributes nearly 49% of the Yellow River's total discharge, making it one of China's most important water sources. However, within the national surface water quality monitoring network, only four sites (M1–M4) are situated at the headwaters of the Yellow River (Fig. 1b).

https://doi.org/10.5194/egusphere-2026-731
Preprint. Discussion started: 19 February 2026

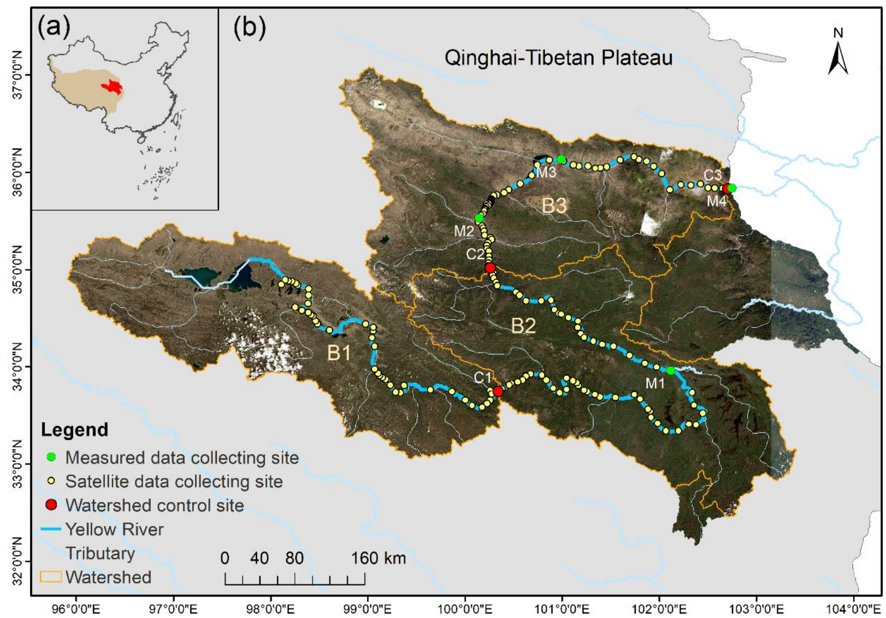

Fig.1 Location of the source region of the Yellow River (a), river network within the study area and data collection sites along the mainstream of the Yellow River (b). B1–B3 represent the up-, mid-, and downstream region of the Yellow River's headstream. A total of 160 monitoring sites span from downstream to upstream, with Site 1 located at the basin outlet.

2.2 Data collection

2.2.1 In-situ Water Quality Data

Riverine COD data for model training were obtained from 107 monitoring sites distributed across the QTP and surrounding regions (Fig. S2), including four sites (M1–M4) positioned along the mainstream of the Yellow River (Fig. 1b). COD data for each site was obtained from the China National Environmental Monitoring Centre (CNEMC; https://www.cnemc.cn/) for the period 2021–2023. Measurements were performed every four hours (00:00, 04:00, 08:00, 12:00, 16:00, and 20:00). Following the *Environmental Quality Standards for Surface Water* (GB 3838–2002),

https://doi.org/10.5194/egusphere-2026-731
Preprint. Discussion started: 19 February 2026

COD was determined using the acidic potassium permanganate method, in which 50 ml water sample was oxidized by standardized $KMnO_4$ solution under controlled heating conditions. After the reaction, the residual permanganate was titrated, and COD_{mn} was calculated from the amount of $KMnO_4$ consumed.

2.2.2 Satellite Reflectance Data

Surface reflectance data for model training was acquired for the 107 monitoring sites across the QTP and its surrounding areas from 2021 to 2023 using the Google Earth Engine (GEE) platform, based on Landsat-8 OLI/TIRS and Landsat-9 OLI-2/TIRS-2 imagery. For historical COD estimation in the source region of the Yellow River, surface reflectance data from Landsat-8 OLI/TIRS was also collected for 2014–2024 at 160 sites located at the headwater of the Yellow River (Fig. 1b). The Landsat-8/9 OLI datasets include five visible and near-infrared (VNIR) bands and two shortwave infrared (SWIR) bands (J. Li et al., 2025). Atmospheric correction for Landsat-8 and Landsat-9 imagery was performed using the Land Surface Reflectance Code (LaSRC, version 1.5.0). Pixels affected by clouds, cloud shadows, snow, ice, or non-water surfaces were removed based on the Landsat reflectance quality assessment bands.

2.2.3 Geographical Feature Data

Monthly precipitation and temperature data were obtained from the 1-km *Monthly Precipitation Dataset for China* (1901–2024) (Peng, 2025a, 2025b). Surface soil properties, including soil texture, pH, soil organic carbon, and bulk density, were extracted from the *Harmonized World Soil Database* (FAO, 2021). Vegetation coverage data were sourced from the *China Regional 250-m Fractional Vegetation Cover Dataset* (2000–2024) (Gao et al., 2025). Land use data were derived from the *Land Use Dataset of China* (1980–2015) provided by the Resource and Environmental

https://doi.org/10.5194/egusphere-2026-731
Preprint. Discussion started: 19 February 2026

Science Data Center, Chinese Academy of Sciences (2020). Human Activity Intensity Index (HAII) were obtained from the *Human Activity Intensity Dataset of the Qinghai–Tibet Plateau* (2000–2020) (Liu, 2023). The Human Activity Intensity Index was calculated based on key human activity data, including agricultural and animal husbandry practices, industrial and mining development, urbanization, tourism, major ecological engineering projects, and pollutant discharge. Digital Elevation Model (DEM) data were retrieved from https://viewfinderpanoramas.org. Historical and projected Yellow River discharge data were compiled from previously published studies (Long et al., 2024; L. Liu et al., 2025; M. Ma et al., 2023; Wang, 2024).

Future monthly temperature and precipitation data with spatial resolution of 1 km in the Yellow River source region were obtained from climate projections generated by the Beijing Climate Center Climate System Model, version 2 (BCC-CSM2-MR) (Hu et al., 2025). This data was generated under three Shared Socioeconomic Pathways (SSPs) aligned with climate scenarios: SSP126 (sustainability-focused, low radiative forcing), SSP245 (intermediate, moderate stabilization), and SSP585 (fossil-fueled development, high radiative forcing).

2.3 Model Development for Historical COD Reconstruction

2.3.1 Matching Measured COD with Satellite Reflectance

COD data and satellite reflectance data (Landsat-8 OLI/TIRS and Landsat-9 OLI-2/TIRS-2) acquired from 107 sites across the eastern QTP and adjacent regions during 2021–2023 were used for model development (Fig. S2). Since Landsat-8/9 overpasses the study region at approximately 10:30 local time, COD measurements obtained at 08:00 or 12:00 on the same day were paired with corresponding satellite scenes. When multiple valid matches were available, only the 12:00

https://doi.org/10.5194/egusphere-2026-731
Preprint. Discussion started: 19 February 2026

COD measurement was retained to ensure temporal consistency. A total of 3048 valid COD–reflectance matchups were obtained for the 107 sites during 2021–2023. These matched datasets covered a broad COD concentration range (0.25–23.2 mg L^{-1}) and were used to develop models for COD prediction.

2.3.2 Input and Prediction Variables of Models

The 3048 valid COD–reflectance matchups were further processed to generate input variables. Input features included raw spectral bands and derived indices, with COD serving as the prediction variable. The raw spectral bands comprised Landsat-8/9 reflectance from Bands 1–7 and selected band ratios (SR_{nir}/SR_{red}, SR_{red}/SR_{green} and SR_{red}/SR_{blue}). Additionally, several spectral indices known to be sensitive to organic matter were calculated (Table S1), namely the Normalized Difference Chlorophyll Index (NDCI), Organic Carbon Index (OC_Index), Normalized Suspended Material Index (NSMI), and Hue Angle (Yan et al., 2025b). Longitude and latitude were also incorporated as input variables.

2.3.3 Model Training

The AutoGluon-Tabular algorithm, implemented in the Anaconda3 environment, was employed to train models for COD prediction with Landsat-derived spectral features mentioned above. AutoGluon-Tabular is an open-source automated machine learning (AutoML) framework that builds high-accuracy predictive models for tabular data through multi-layer model ensembling and stacking. AutoGluon's *TabularPredictor* was configured in regression mode and trained using multiple base learners (e.g., Gradient Boosting Machines, Random Forests, Neural Networks). The framework automatically optimized model selection, hyperparameters, and ensemble weights. The matched dataset (3048 pairs) described in Section 2.3.2 was randomly divided into training

https://doi.org/10.5194/egusphere-2026-731
Preprint. Discussion started: 19 February 2026

(80%) and testing (20%) subsets. A total training time limit of 600s was assigned to ensure sufficient exploration of model configurations.

2.3.4 Model Evaluation

Model performance was evaluated using the negative Root Mean Squared Error (RMSE) for both the validation and test datasets (Eqs. 1–2). Lower (i.e., closer-to-zero) test and validation scores indicated superior model performance. The performance metrics for all models are summarized in Table S2.

$$RMSE = \sqrt{\frac{1}{n}\sum_{i=1}^{n}(y_i - \hat{y}_i)^2} \qquad (1)$$

$$\text{Test /Validation score} = -RMSE \qquad (2)$$

where, N denotes the size of the observations and y_i and $\hat{y}_i$ denote the in-situ values and satellite-retrieved values, respectively.

The importance of different input variables affecting the prediction of COD was also assessed based on the importance scores (Eq.3).

$$Importance\ (f_i) = M(D) - M(D_{\_shuffled(f_i)}) \qquad (3)$$

where, $M(\cdot)$, model performance metric (e.g., accuracy, log-loss, RMSE); D, original evaluation dataset; $D_{shuffled(fi)}$, same dataset, but with feature f_i randomly permuted; *Importance(fi)*, Drop in performance when f_i is destroyed.

2.3.5 Reconstruct of Historical COD and Calculation of COD Changes

The model exhibiting the highest test and validation scores was applied to reconstruct COD concentrations at 160 sites located in the headwater region of the Yellow River from 2014 to 2024 using Landsat-8 surface reflectance data. To evaluate model applicability and reliability, the reconstructed COD concentrations were compared with in situ measurements at two representative headwater sites. Model accuracy was assessed for the two sites using the Mean Absolute Percentage Difference (MAPD), RMSE, and Bias, following the approach of Yan et al. (2025). Historical COD changes were assessed by comparing averages from 2014–2015 and 2023–2024.

2.4 Prediction of Future COD and Its Changes in the Headstream of the Yellow River

To predict future COD levels at 160 sites in the headwaters of the Yellow River, the machine learning approach was also employed to model the relationships between geographical variables and the satellite-based estimates of COD levels. Using the Anaconda3 platform, soil texture (sand, silt, clay), bulk density, soil organic carbon, soil pH, altitude, human activity intensity, vegetation cover, land use, and ten-year averages of annual mean precipitation and temperature for each site during 2014-2024 were used as input features, while the ten-year average COD concentration for each site during 2014-2024 served as the target variable. The best-performing model, selected based on test and validation scores, was then used to predict future COD concentrations, incorporating both static variables (e.g., soil properties, vegetation cover, land use) and dynamic variables (future annual mean precipitation and temperature), depending on data availability.

In order to predict the future COD using the trained model, future monthly temperature and precipitation data was collected from Hu et al., (2025). Future annual mean precipitation and temperature were then calculated for 2025-2040, 2041-2070, and 2071-2100, representing near-, mid-, and long-term horizons. Future COD changes in the Yellow River source region for 2025-2040, 2041-2070, and 2071-2100 under SSP126, SSP245, and SSP585 scenarios were calculated relative to the mean values from 2014–2024.

2.5 Calculation of COD flux

The COD flux in the source region of the Yellow River was calculated using Eq. 4:

https://doi.org/10.5194/egusphere-2026-731
Preprint. Discussion started: 19 February 2026

$$F = C_i \times Q_i/10 \tag{4}$$

where, F (Gg), nutrient export; C_i (mg/L), COD concentration; Q_i (10^8 m³), river discharge.

3 Results

3.1 Performance of developed models

3.1.1 Predicting Historical COD Using Landsat Reflectance Data

A total of 24 models were developed and evaluated on the Anaconda3 platform to predict COD levels from Landsat reflectance data, with test and validation scores summarized in Table S2. The LightGBMLarge model demonstrated the highest predictive accuracy for COD across the QTP and surrounding regions, achieving test and validation scores of –0.22325 and –0.66913, respectively. Predicted versus in-situ measured COD levels for 2021–2023 based on training dataset are shown in Fig. 2a, with RMSE and R^2 of 0.326 and 0.925, respectively, indicating strong predictive performance.

The relative importance of input variables in the LightGBMLarge model was quantified using importance scores (Fig. 2b). The five most influential predictors were longitude, latitude, SR_{Red}/SR_{Green}, NSMI, and Band 1. Based on its performance, the LightGBMLarge model was selected to estimate historical COD levels in the source region of the Yellow River.

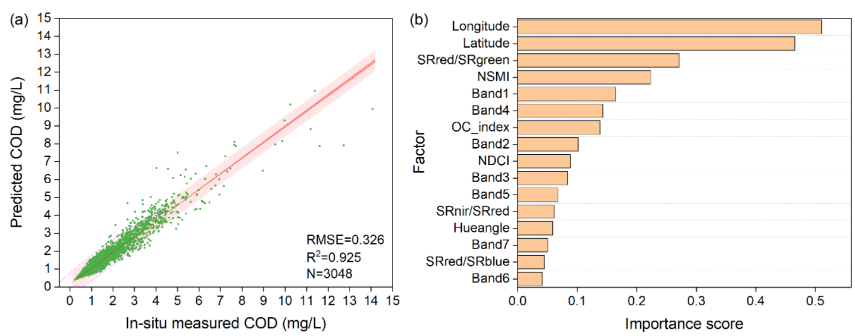

Fig.2 Model performance for COD prediction based on training set using Landsat 8/9 reflectance

https://doi.org/10.5194/egusphere-2026-731
Preprint. Discussion started: 19 February 2026

data (a), and importance of input variables in COD prediction (b). Bands 1-7 are surface reflectance data produced by the Landsat 8 OLI/TIRS sensors; SR_{nir}/SR_{red}, SR_{red}/SR_{green} and SR_{red}/SR_{blue} are band ratios; NSMI is Normalized Suspended Material Index; OC_Index is Organic Carbon Index; NDCI is Normalized Difference Chlorophyll Index; Hue Angle is used to reflect watercolor and water quality.

To assess model reliability in the study area, two representative sites (M2 and M3) in the Yellow River headwaters were used to compare modeled and in-situ COD time series (Fig. 3). The results indicate that the model can accurately capture both spatial and temporal variability of riverine COD in the headstreams of the Yellow River. At site M3, RMSE, MAPD, and Bias were 0.12 mg L^{-1}, 8.16%, and –2.38%, respectively, and RMSE, MAPD, and Bias at site M2 were 0.58 mg L^{-1}, 15.32%, and –2.23%, respectively.

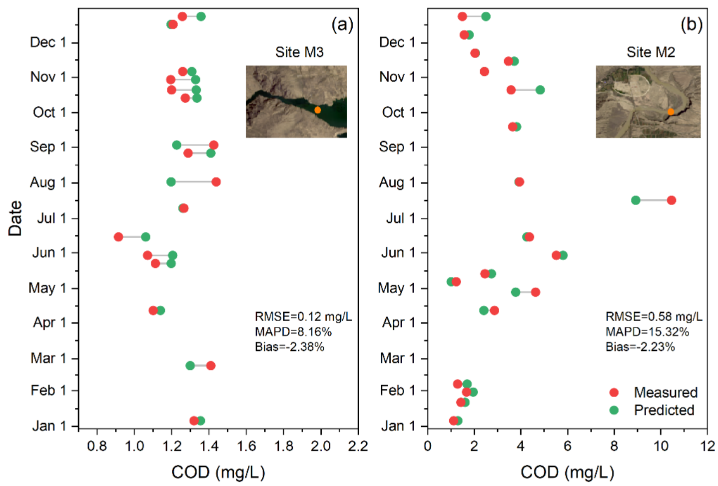

Fig.3 Comparison between predicted and measured COD values in 2023 at sites M3 (a) and M2 (b) within the Yellow River source region. For sites M2 and M3, 24 and 20 matched data points were collected, respectively.

https://doi.org/10.5194/egusphere-2026-731
Preprint. Discussion started: 19 February 2026

3.1.2 Prediction of Future COD Using Geographical Features

Models for predicting future COD based on geographical features were also developed using the Anaconda3 platform. A total of 36 models were evaluated (Table S3), and the LightGBMLarge model exhibited the highest performance, with test and validation scores of –0.081 and –0.264, respectively. Predicted versus satellite-based estimates of average COD levels based on the training dataset in the Yellow River source region are presented in Fig. 4a, achieving an R^2 of 0.913 and an RMSE of 0.177, indicating strong predictive capability of this model. Analysis of feature importance revealed that altitude, precipitation, temperature, and vegetation contributed most significantly to COD variability in the study area (Fig. 4b).

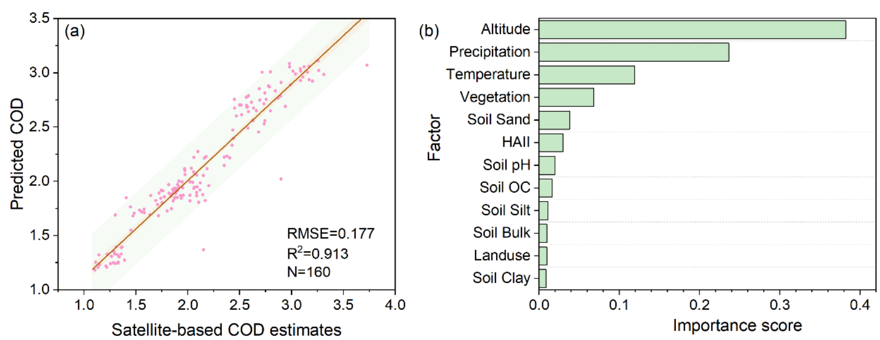

Fig.4 Performance of the developed model for COD prediction based on the training set using geographical feature data (a), and importance of variables in the predictive model (b). HAII is Human Activity Intensity Index; Soil OC represents soil organic carbon; Soil Bulk is soil bulk density; Soil Sand, Clay and Silt are soil texture.

3.2 Spatiotemporal Changes of COD in the Headstream of the Yellow River

The developed model estimated an annual mean COD concentration of 2.14 ± 1.06 mg L^{-1} in the

https://doi.org/10.5194/egusphere-2026-731
Preprint. Discussion started: 19 February 2026

Yellow River source region from 2014 to 2024, with pronounced spatial variability. In the upstream area, the mean COD was 1.89 ± 0.81 mg L⁻¹, while higher concentrations were observed in the mid-downstream region (2.73 ± 1.63 mg L⁻¹). The downstream area, which includes large reservoirs such as Longyangxia and Lijiaxia, exhibited significantly lower COD levels (1.54 ± 0.50 mg L⁻¹) (Fig. 5a,b).

Over the past decade, the midstream region showed a clear increasing trend in COD, with an average rise of 0.441 mg L⁻¹ (Fig. 5c,d). In contrast, the upstream area exhibited both increasing and decreasing trends, with a mean change of 0.099 mg L⁻¹, whereas COD concentrations in the downstream region remained relatively stable (mean change: –0.002 mg L⁻¹).

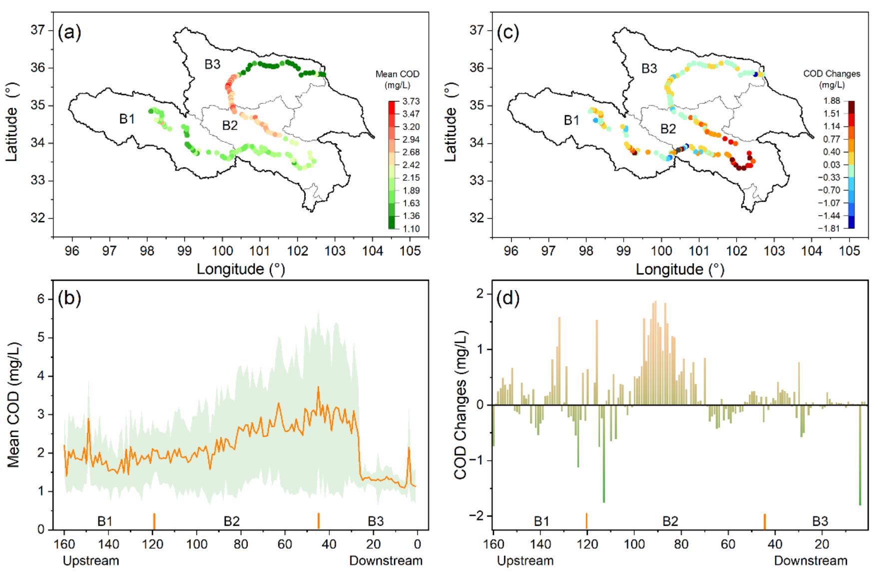

Fig.5 Spatial variation of mean COD and its change between 2014–2024 in the Yellow River source region. Changes were assessed by comparing averages from 2014–2015 and 2023–2024.

Seasonal variations of COD were also evident during our study. Average monthly COD

https://doi.org/10.5194/egusphere-2026-731
Preprint. Discussion started: 19 February 2026

concentrations ranged from 0.8 to 8 mg L⁻¹ (Fig. 6). The downstream site maintained low (0.8-2.4 mg L⁻¹) and showed higher COD levels in summer (Fig. 6a), while the midstream site exhibited a pronounced increase from March, peaking in July (~8 mg L⁻¹), followed by a gradual decline (Fig. 6b). The upper–midstream site displayed two distinct peaks in late spring and summer, suggesting episodic organic inputs associated with ice melt and rainfall (Fig. 6c). Upstream sites remained low to moderate (1-3 mg L⁻¹) with minimal seasonal variation (Fig. 6d).

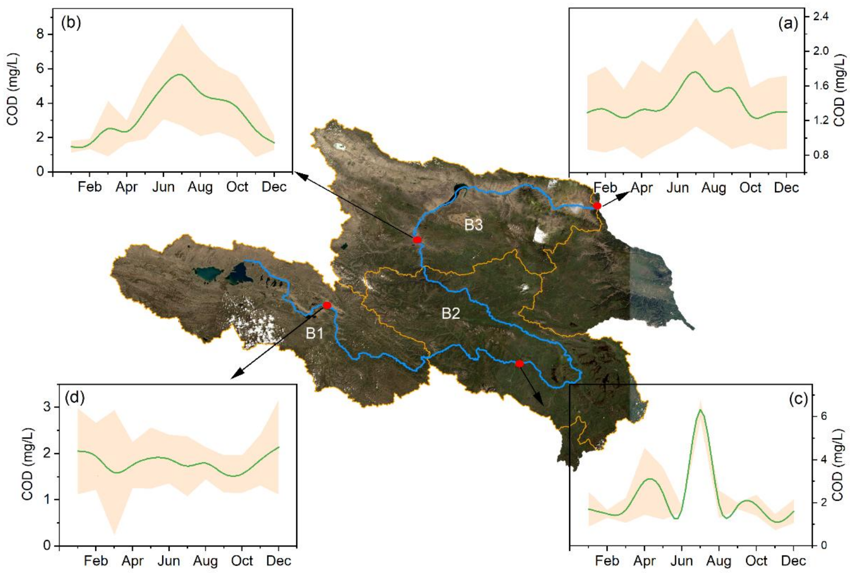

Fig.6 Averaged monthly variations of COD during 2014–2024 within the Yellow River source region.

3.3 Future Climate and COD Changes in the Source Region of the Yellow River

Across all scenarios and periods, precipitation exhibits a consistent spatial pattern, increasing from upstream reaches to a midstream maximum and subsequently decreasing toward downstream

https://doi.org/10.5194/egusphere-2026-731
Preprint. Discussion started: 19 February 2026

sections (Fig. 7a-c). This pattern is preserved under all SSPs, although the magnitude of precipitation varied among scenarios and time slices. Relative to current conditions, precipitation increases slightly in the midstream region under SSP126 and SSP245, particularly during the mid- and late-century periods. Under SSP585, precipitation displays enhanced increase, with higher midstream values during 2041–2070 and 2071–2100 and lower precipitation toward downstream reaches.

Compared with current conditions, future temperature rises across the entire study area (Fig. 7d-f), with the magnitude of warming increasing over time and from SSP126 to SSP585. Under SSP126, temperature increases are relatively moderate, whereas SSP245 shows stronger warming, especially during 2071–2100. The largest temperature increases occurred under SSP585, with pronounced downstream variability during the late-century period, resulting in an amplified longitudinal temperature gradient.

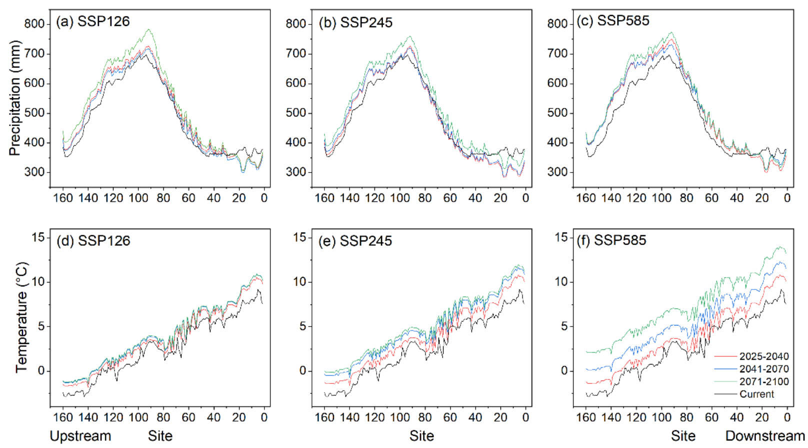

Fig.7 Projected precipitation and temperature variations for 2025-2040, 2041-2070, and 2071-2100 under SSP126, SSP245, and SSP585 scenarios based on CMIP6 data.

https://doi.org/10.5194/egusphere-2026-731
Preprint. Discussion started: 19 February 2026

Projected changes in COD across the study area show pronounced spatial and temporal variability under all three SSP scenarios (Fig. 8). During the near-term period (2025–2040), COD changes are generally modest, with most monitoring sites exhibiting values close to zero. In the mid-term period (2041–2070), the COD changes show an overall increase, with mean value of 0.05 mg L⁻¹. Specifically, midstream sites more frequently experience decreases in COD, whereas upstream and downstream regions display a mixture of small increases and decreases. By the late-century period (2071–2100), the average change in COD is -0.01 mg L⁻¹. COD shows a pronounced decrease trend in the midstream area (-0.12 mg L⁻¹) under SSP585. Upstream and downstream areas show a higher occurrence of positive COD changes. Overall, COD shows a slight increasing trend across the three scenarios over different periods, with 877 positive changes (61%) and 563 negative changes (39%).

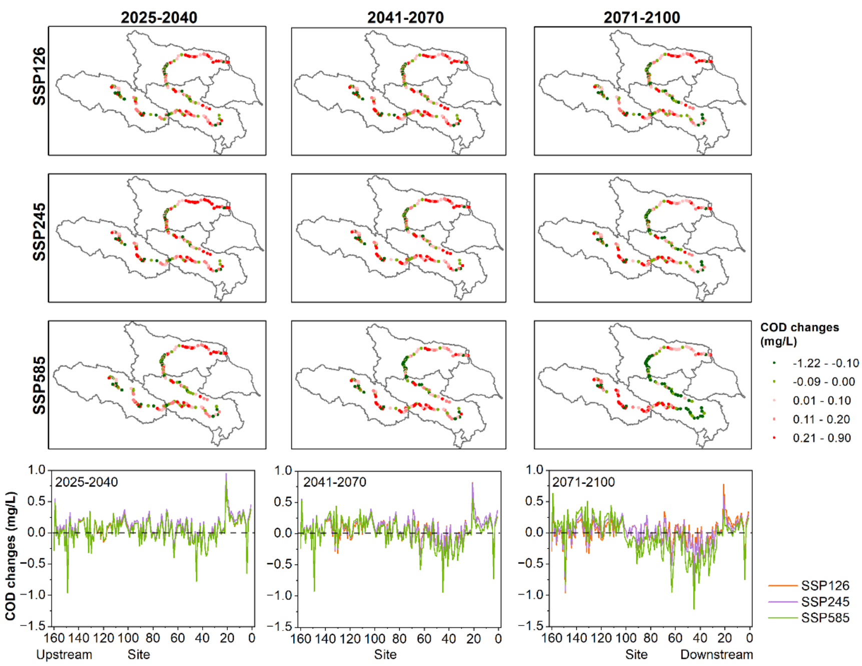

Fig.8 Projected spatial variation of COD changes in the Yellow River source region for 2025-2040,

https://doi.org/10.5194/egusphere-2026-731
Preprint. Discussion started: 19 February 2026

2041-2070, and 2071-2100 under SSP126, SSP245, and SSP585 scenarios. COD changes were calculated relative to the mean values from 2014–2024.

3.4 Historical and Future COD Exports in the Source Region of the Yellow River

Based on the annual average discharge at control site C3 (1987–2021), approximately 28.1 Gg of COD was exported from the entire study area. In contrast, the annual mean COD export at site M2 was 62.5 Gg, indicating that approximately 34 Gg of COD was either deposited or decomposed between C3 and M2 along the downstream of the Yellow River's source region. The export of COD primarily occurred during the wet season (June–October) (Fig. 9a), which contributes substantially to the annual COD export from the source region (Fig. 9b). Additionally, the observed increase in COD export between sites M1 and M2 highlights the midstream region as a major source of COD (Fig. 9b).

Affected by the increase in the projected runoff (Fig. 9c), future projections at site M2 indicate a slight declining trend in COD export from 2025 to 2100 under SSP126 scenarios, and an increase trend under SSP245 and SSP585 scenarios (Fig. 9d). By 2100, the average COD export at M2 under different scenarios is expected to increase from 62.5 to 81.6 Gg.

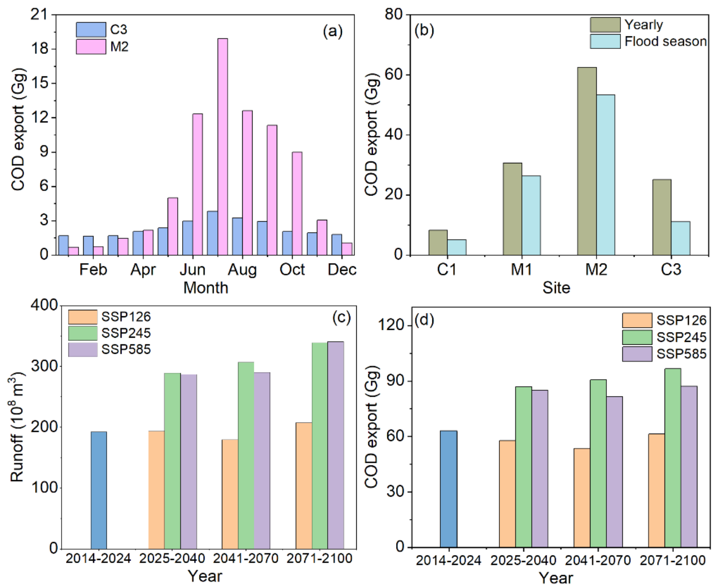

Fig.9 Monthly average COD export during 2014-2024 at sites M2 and C3 (a); comparison of annual average COD export and flood-season COD export during 2014-2024 among sub-basins (b); projected annual runoff (c) and COD export at M2 for 2025-2040, 2041-2070, and 2071-2100 under SSP126, SSP245, and SSP585 scenarios (d). C1–C3 are the control sites for sub-basins B1–B3, respectively. Historical annual and seasonal runoff was obtained from L. Liu et al. (2025) and Wang (2024). The projected runoff under SSP126 was derived from M. Ma et al. (2023), while the runoff under SSP245 and SSP585 was calculated using data from Long et al. (2024). Different sources of runoff data may result in discrepancies in the predicted COD exports across scenarios.

4 Discussion

4.1 Factors Driving COD Dynamics in the Headstream of the Yellow River

4.1.1 Spatial Variations

Primary sources of riverine organic carbon include losses from soils, plant litter, root exudates in

https://doi.org/10.5194/egusphere-2026-731
Preprint. Discussion started: 19 February 2026

grasslands, and permafrost thaw via surface runoff (Yan et al., 2023). In this study, precipitation, temperature, vegetation, and soil texture were identified as key drivers of COD variation (Fig. 4b). Notably, the overall soil organic carbon, vegetation cover, fine particle content, and precipitation are higher in the midstream region of the headwater (Fig. S3), providing abundant carbon sources and facilitating transport to nearby rivers, resulting in elevated COD levels and fluxes in the mid-downstream areas (Figs. 5a, 9a,b). Additionally, bare land in the mid-downstream areas of the headstream may also contribute to the soil erosion and the associated organic carbon losses (Fig. S1). L. Li (2025) identified the higher lateral fluxes of river organic matter in the midstream area of the Yellow River' s source region. Consequently, the midstream area represents a critical source of organic carbon for the Yellow River headwaters.

In contrast, COD levels decreased markedly in the downstream region (Figs. 5a,b). This decline is likely driven by damming, as three large reservoirs, Longyangxia, Laxiwa, and Lijiaxia have been constructed in the downstream headwater region since the 1970s. Reservoirs increase water residence time, promoting deposition and decomposition of organic carbon, greenhouse gas emissions, and uptake by aquatic plants (Maavara et al., 2017, 2020). Therefore, the deposition or decomposition of organic matter along the downstream areas may contribute to the decline of COD levels. The deposition of riverine organic matter can be inferred from the decrease in COD fluxes at the outlet (C3) of the study area relative to Site M2 (Figs. 9a, b). L. Li et al. (2025) also reported negative dissolved organic matter fluxes in the main channels of the Yellow River's headstreams. Additionally, the decomposition of the deposited organic matter is evidenced by CO_2 outgassing from the river water. Previous study has found that CO_2 outgassing from the cascade reservoirs of Yellow River's source region was estimated at 131.02 ± 156.77 mmol m^{-2} d^{-1} in dry

https://doi.org/10.5194/egusphere-2026-731
Preprint. Discussion started: 19 February 2026

seasons and 466.10 ± 366.67 mmol m⁻² d⁻¹ in flood seasons (Wang et al., 2022). Therefore, these observations suggest that the sedimentation and degradation of organic matter contributes to lower COD concentrations in the downstream area.

The COD concentration remained relatively stable along the upper to middle reaches of the Yellow River's headwaters. This region is characterized by permafrost and seasonally frozen ground, with low precipitation and limited runoff (Yang et al., 2023). Surface runoff in this area primarily originates from precipitation, snowmelt, and glacier melt (G. Li et al., 2025). Consequently, due to the relatively uniform and stable runoff and land cover, COD levels exhibited a homogeneous spatial distribution along the upper to middle reaches of the Yellow River's headwaters.

4.1.2 Temporal Variations

Climate-driven changes in runoff and temperature strongly influence catchment-scale carbon dynamics, altering riverine organic matter fluxes globally (Costa et al., 2023). Over the past decade, air temperature in the source region of the Yellow River has shown an increasing trend, with a basin–averaged increase of 0.67 °C, and the precipitation also presented an over increase trend though decrease slightly after 2019 (Fig. S4). The study area is particularly sensitive to warming-induced permafrost thaw, glacier melting, soil erosion, and intensified human activities over recent decades (Chen et al., 2022; Deng et al., 2025; Lan et al., 2025), which modify ROM sources and lateral transport between terrestrial and aquatic systems, affecting ROM levels and fluxes in rivers (Chen et al., 2022; Wang et al., 2020, 2025). Previous studies highlighted that permafrost thaw was projected to release 129.39 ± 21.02 Tg soil organic carbon annually (Lan et al., 2025). Glacier melting contributes an estimated 0.19 Tg C yr^{-1} as dissolved organic carbon

https://doi.org/10.5194/egusphere-2026-731
Preprint. Discussion started: 19 February 2026

(Chen et al., 2022). Intensified rainfall has increased soil erosion by 42% over the past four decades, resulting in an average soil carbon loss of 4 ± 1.2 Tg C yr^{-1} (Deng et al., 2025).

Therefore, affected by the increased temperature and precipitation, COD concentrations in the source region of the Yellow River exhibited an overall increasing trend over the past decade, with an average rise of 0.186 mg L^{-1} (Figs. 5c,d). Especially the midstream region experienced the most pronounced increase (0.441 mg L^{-1}). The higher precipitation combined with increased runoff likely enhance organic matter leaching from grasslands, contributing to the rise of riverine COD in the midstream area (Chen et al., 2025; Yang et al., 2023).

In addition to climate effects, growing human activities such as land use changes, grazing, and construction on the QTP also influence carbon mobilization (Chen et al., 2022). Human-induced land-use changes, grassland degradation, construction activities, and overgrazing can lead to organic matter losses in the study area. In addition, the construction and urbanization of natural and agricultural ecosystems may further accelerate organic matter losses within the watershed. All these human activities may contribute to the rising of COD in the headstream of the Yellow River.

4.2 Future Changes in COD under Climate Change

Rapid climate change in alpine regions is altering carbon cycling in both terrestrial and aquatic ecosystems (Chen et al., 2022). As carbon dynamics are highly sensitive to climatic variations, warming and wetting trends are expected to influence the stability of riverine organic matter in alpine catchments. Numerous studies indicate that precipitation and temperature on the QTP are projected to increase throughout this century, particularly in high-elevation areas (Karim et al., 2025; Meng et al., 2023). Our projections also suggest an overall increase in precipitation,

https://doi.org/10.5194/egusphere-2026-731
Preprint. Discussion started: 19 February 2026

especially in the up-midstream area of the Yellow River source region (Fig. 7), and significant warming is projected in the whole study area by 2100, especially under SSP 245 and SSP585.

Climate-driven changes are expected to induce the largest variability in COD concentrations in the midstream region (Fig. 8). COD levels are projected to increase in most parts of the source region of the Yellow River, and annual average COD exports will increase from 62.5 Gg to 81.6 Gg (Fig. 9d). ROM dynamics are jointly regulated by organic matter supply and hydrological processes within catchments (Li et al., 2022; Wu et al., 2024). Increased precipitation can enhance surface runoff, leading to losses of organic matter from the catchment, even though COD concentrations may be diluted as discharge continues to increase (Li et al., 2022; Wu et al., 2024). The projected warming in the headwater area of the Yellow River will lead to the continuing permafrost degradation, promoting the loss of organic matter within the catchment and leading to the increase of the COD level in the headstreams (Z. Li et al., 2025). In addition, damming prolongs water residence time, promoting organic matter deposition in cascade reservoirs in the downstream area of the Yellow River's source region. Under warm conditions, the degradation of deposited organic matter in the bottom of the reservoir may be enhanced, releasing additional organic carbon from reservoir sediments and contributing to the rise of COD levels in the downstream area (Battin et al., 2023; Vachon et al., 2021).

However, the extent to which organic matter reaches rivers depends on hydrological processes and connectivity between the source region and river channels. The characteristics of rainfall events may shift the ROM response to storms from transport-limited to supply-limited, thereby reducing ROM levels (Li et al., 2022). Consequently, the projected increase in precipitation by the 2100s is expected to lead to a decrease in COD levels within the midstream

https://doi.org/10.5194/egusphere-2026-731
Preprint. Discussion started: 19 February 2026

areas (Fig. 8). In addition, permafrost thaw induced by the warming can also alter runoff pathways, promoting subsurface flow and potentially reducing surface discharge to rivers (Yang et al., 2023). Increased vegetation cover can also reduce transport of organic matter through reducing soil erosion and surface runoff (Liu et al., 2024; W. Ma et al., 2023). Therefore, these factors may jointly contribute to the decrease of riverine organic matter at some specific sites on the headstream of the Yellow River.

4.3 Uncertainty in Riverine Organic Matter Dynamics on the QTP

Understanding riverine organic matter dynamics is essential for assessing aquatic ecosystem feedback to climate change. Ongoing warming and wetting on the QTP are expected to alter carbon stability, increasing uncertainty in watershed organic matter losses (Bai et al., 2025). For instance, increased precipitation may enhance surface runoff (Li et al., 2022), however, rising temperatures can also decrease catchment runoff by enhancing evaporation. The influence of hydrological processes on ROM dynamics depends on the characteristics of the catchment (Li et al., 2022). Previous studies have predicted both increasing and decreasing streamflow trends on the QTP under future climate scenarios (G. Li et al., 2025; San et al., 2025; Yang et al., 2023). Increased streamflow may elevate COD in rivers, or dilute COD due to higher streamflow. Conversely, reduced streamflow may decrease organic matter transport to rivers or concentrate COD in river water.

Additionally, warming-induced permafrost thaw may accelerate topsoil organic matter mobilization, stimulate microbial activity, and promote soil organic matter decomposition, releasing more dissolved organic matter (Z. Li et al., 2025). However, the frozen ground degradation can also result in the decreased surface runoff by increasing the subsurface runoff

https://doi.org/10.5194/egusphere-2026-731
Preprint. Discussion started: 19 February 2026

(Yang et al., 2023). Vegetation greening on the QTP may both enhance soil carbon storage and reduce organic matter losses to river networks through mitigating soil erosion (Deng et al., 2025). Therefore, climate change can further differentially affect terrestrial carbon stocks and carbon losses, introducing additional complexity and uncertainty in catchment-scale organic matter sources and transport (Chen et al., 2022; Liu et al., 2024; W. Ma et al., 2023).

In-stream carbon biogeochemical processes are also highly complex under changing climatic conditions. Organic matter decomposition depends on temperature, redox conditions, hydrology, microbial activity, and organic matter characteristics (Battin et al., 2023). The climate change is projected to change the hydrological processes and the associated biogeochemical processes, further altering the carbon cycling in the alpine rivers. However, interactions among these factors are not fully understood in alpine rivers, making predictions of alpine river metabolism and carbon budget under climate change uncertain (L. Li et al., 2025).

Anthropogenic activities on the QTP further contribute to uncertainty. Warming and wetting may expand farming, increasing soil erosion and carbon losses (Chen et al., 2022). Future dam construction alters organic matter transport by promoting deposition, influencing greenhouse gas emissions, and facilitating organic matter degradation (Battin et al., 2023). Conversely, ecological restoration, such as afforestation, can increase soil organic matter accumulation and litterfall (Chen et al., 2022; Yan et al., 2023), leading to increase in organic matter and the COD levels in the nearby headwaters of the Yellow River.

In this study, we project a general increase in levels and fluxes of COD based on modeled temperature, precipitation, and discharge. However, future climatic trends may deviate from current projections, and the predicted temperature and precipitation may not represent the actual

https://doi.org/10.5194/egusphere-2026-731
Preprint. Discussion started: 19 February 2026

future patterns. Furthermore, our developed model does not incorporate changes in land covers, soil carbon stocks, hydrological processes, or in-stream carbon biogeochemistry, all of which may significantly influence riverine carbon cycling. Therefore, future research should integrate these factors to develop more precise, process-based models and improve understanding of carbon dynamics in alpine river catchments.

5 Conclusions

In this study, LightGBM-Large models were developed to reconstruct the historical variations of COD in the source region of the Yellow River and to predict its future changes. Our findings identify the midstream region of the Yellow River's headstream, with higher COD levels (2.73 ± 1.63 mg L^{-1}), is sensitive to climate change and exhibited an increasing trend of COD (+0.44 mg L^{-1}) in the past decade. Precipitation and temperature were identified as the key factors influencing COD dynamics in the headwaters of the Yellow River. Future projections suggest that increased precipitation and temperature may lead to an overall rise of COD levels, with decrease in some specific sites. The export of organic matter from the headwaters of the Yellow River is also projected to increase based on the anticipated increase in COD levels and discharge. However, the limited spatial and temporal resolution of Landsat data and lack of geophysical data, still poses challenges for accurately capturing rapid variations in riverine COD in the source region of the Yellow River. Therefore, future research should focus on developing more robust models by integrating higher-quality satellite observations and incorporating a broader range of environmental variables.

Data availability

The data will be available upon request.

Author contributions

XW: Conceptualization, Methodology, Writing–original draft, Funding acquisition; JW: Methodology, Data curation, Review and editing; TR: Investigation, Formal analysis, Validation; JZ: Validation, Conceptualization, Review and editing.

Competing interests

The authors declare that they have no conflict of interest.

Acknowledgments

We thank the National Tibetan Plateau / Third Pole Environment Data Center and Google Earth Engine for providing data.

Financial support

This work was funded by China West Normal University (22kA001, 17E040, CXTD2020-3).

References

Adegun, A., Viriri, S., Tapamo, J.-R., 2023. Review of deep learning methods for remote sensing satellite images classification: experimental survey and comparative analysis. Journal of Big Data 10. https://doi.org/10.1186/s40537-023-00772-x

Aryal, S., Pokhrel, Y., 2025. Spatio-temporal heterogeneities in hydrologic dynamics across the Asian Water Tower. Journal of Hydrology 662, 133951. https://doi.org/10.1016/j.jhydrol.2025.133951

Bai, Y., Peng, Y., Zhang, D., Yang, G., Chen, L., Kang, L., Zhou, W., Wei, B., Xie, Y., Yang, Y., 2025. Heating up the roof of the world: tracing the impacts of in-situ warming on carbon cycle in alpine grasslands on the Tibetan Plateau. National Science Review 12, nwae371.

Battin, T.J., Lauerwald, R., Bernhardt, E.S., Bertuzzo, E., Gener, L.G., Hall, R.O., Hotchkiss, E.R.,

https://doi.org/10.5194/egusphere-2026-731
Preprint. Discussion started: 19 February 2026

Maavara, T., Pavelsky, T.M., Ran, L., Raymond, P., Rosentreter, J.A., Regnier, P., 2023. River ecosystem metabolism and carbon biogeochemistry in a changing world. Nature 613, 449–459. https://doi.org/10.1038/s41586-022-05500-8

Chen, H., Ju, P., Zhu, Q., Xu, X., Wu, N., Gao, Y., Feng, X., Tian, J., Niu, S., Zhang, Y., 2022. Carbon and nitrogen cycling on the Qinghai–Tibetan Plateau. Nature Reviews Earth & Environment 3, 701–716.

Chen, Z., Su, B., Fohrer, N., Huang, J., Zhao, M., Wen, S., Jiang, T., 2025. Response of discharge in the Upper Yellow River Basin to changing climate over the long time period (1850–2023). Journal of Water and Climate Change 16, 655–674.

Chinese Academy of Sciences Resource and Environmental Science Data Center, 2020. Landuse dataset in China (1980-2015). National Tibetan Plateau Data Center.

Costa, D., Sutter, C., Shepherd, A., Jarvie, H., Wilson, H., Elliott, J., Liu, J., Macrae, M., 2023. Impact of climate change on catchment nutrient dynamics: insights from around the world. Environ. Rev. 31, 4–25. https://doi.org/10.1139/er-2021-0109

Deng, R., Li, D., Zhao, Y., Walling, D.E., Panagos, P., Borrelli, P., Ciais, P., Huang, Y., Bai, Y., Chalov, S., Golosov, V.N., Fu, X., Miao, C., Wei, J., Ni, J., 2025. Intensified rainfall overrides vegetation greening in driving erosion and carbon loss on the Tibetan Plateau. Science Bulletin. https://doi.org/10.1016/j.scib.2025.09.005

Deng, Y., Zhang, Y., Pan, D., Yang, S.X., Gharabaghi, B., 2024. Review of Recent Advances in Remote Sensing and Machine Learning Methods for Lake Water Quality Management. Remote Sensing 16. https://doi.org/10.3390/rs16224196

Food and Agriculture Organization of the United Nations, I.I. for A.S.A., 2021. China soil map

https://doi.org/10.5194/egusphere-2026-731
Preprint. Discussion started: 19 February 2026

based harmonized world soil database (HWSD) (v1.1) (2009). National Tibetan Plateau Data Center.

Gao, J., Shi, Y., Zhang, H., Chen, X., Zhang, W., Shen, W., Xiao, T., Zhang, Y., 2025. China regional 250m fractional vegetation cover data set (2000-2024). National Tibetan Plateau Data Center. https://doi.org/10.11888/Terre.tpdc.300330

Hong, J., Pang, B., Zhao, L., Shu, S., Feng, P., Liu, F., Du, Z., Wang, X., 2025. Soil phosphorus crisis in the Tibetan alpine permafrost region. Nat Commun 16. https://doi.org/10.1038/s41467-025-61501-x

Hotaling, S., Finn, D.S., Joseph Giersch, J., Weisrock, D.W., Jacobsen, D., 2017. Climate change and alpine stream biology: progress, challenges, and opportunities for the future. Biological Reviews 92, 2024–2045. https://doi.org/10.1111/brv.12319

Hu, X., Shi, S., Zhou, B., Ni, J. (2025). A 1 km monthly dataset of historical and future climate changes over China (1991-2100). National Tibetan Plateau / Third Pole Environment Data Center. https://doi.org/10.57760/sciencedb.13546.

Karim, R., Li, S., Su, T., Ayugi, B.O., Babaousmail, H., Xiao, S., 2025. Future Climate Changes on the Qinghai–Tibetan Plateau Under CMIP6 Global Climate Models. International Journal of Climatology e70005.

Kotlarski, S., Gobiet, A., Morin, S., Olefs, M., Rajczak, J., Samacoïts, R., 2023. 21st Century alpine climate change. Clim Dyn 60, 65–86. https://doi.org/10.1007/s00382-022-06303-3

Lan, T., Ma, Q., Lai, Y., Zhang, M., Harbor, J., Luo, X., 2025. Quantifying the water contributions and carbon consequences of permafrost degradation on the Tibetan Plateau. Science Bulletin. https://doi.org/10.1016/j.scib.2025.09.029

https://doi.org/10.5194/egusphere-2026-731
Preprint. Discussion started: 19 February 2026

Li, G., Li, Zongxing, Zhang, B., Li, Zongjie, 2025. Changes in runoff from major alpine watersheds on the Qinghai-Tibetan plateau: A review. Journal of Hydrology: Regional Studies 60, 102514. https://doi.org/10.1016/j.ejrh.2025.102514

Li, J., Wang, G., Li, K., Li, Y., Guo, L., Song, C., 2023. Impacts of climate change and freeze–thaw cycles on water and sediment fluxes in the headwater region of the Yangtze River, Qinghai–Tibet Plateau. CATENA 227, 107112. https://doi.org/10.1016/j.catena.2023.107112

Li, J., Wang, G., Song, C., Sun, S., Ma, J., Wang, Y., Guo, L., Li, D., 2024. Recent intensified erosion and massive sediment deposition in Tibetan Plateau rivers. Nat Commun 15, 722. https://doi.org/10.1038/s41467-024-44982-0

Li, J., Wang, G., Sun, S., Ma, J., Guo, L., Song, C., Lin, S., 2025. Mapping and reconstruct suspended sediment dynamics (1986–2021) in the source region of the Yangtze River, Qinghai-Tibet Plateau using Google Earth Engine. Remote Sensing of Environment 317, 114533. https://doi.org/10.1016/j.rse.2024.114533

Li, L., Wang, T., Yang, J., Yang, H., Tang, L., Yang, D., 2025. Revealing the Long-Term Catchment-Scale Carbon Budget Dynamics on the Permafrost-Dominated Eastern Tibetan Plateau. Global Biogeochemical Cycles 39, e2025GB008743. https://doi.org/10.1029/2025GB008743

Li, X., Wang, J., Lin, J., Yin, W., Shi, Y.Y., Wang, L., Xiao, H.B., Zhong, Z.M., Jiang, H., Shi, Z.H., 2022. Hysteresis analysis reveals dissolved carbon concentration – discharge relationships during and between storm events. Water Research 226, 119220. https://doi.org/10.1016/j.watres.2022.119220

Li, Ziliang, Kang, L., Wang, L., Wanek, W., Zhang, D., Wang, G., Lambers, H., Peñuelas, J., Jiang,

https://doi.org/10.5194/egusphere-2026-731
Preprint. Discussion started: 19 February 2026

M., Yang, Y., 2025. Accelerated soil phosphorus cycling upon abrupt permafrost thaw. Nat. Clim. Chang. https://doi.org/10.1038/s41558-025-02445-4

Li, Z., Zhou, H., Zhang, B., Fa, D., Xue, J., 2023. Hydrologic connectivity between water in permafrost active layer and river water in a small alpine catchment in the northeastern Tibetan Plateau. Applied Geochemistry 154, 105686. https://doi.org/10.1016/j.apgeochem.2023.105686

Li, Z., Liu, F., Li, H., Liu, M., Li, Zongxing, Feng, Q., Xu, B., Liu, X., 2025. Driving forces of the spatiotemporal supply pattern of runoff in the source region of Yellow River. Journal of Hydrology: Regional Studies 60, 102515. https://doi.org/10.1016/j.ejrh.2025.102515

Liu, D., Jiang, X., Duan, M., Yu, S., Bai, Y., 2023. Human and natural activities regulate organic matter transport in Chinese rivers. Water Research 245, 120622. https://doi.org/10.1016/j.watres.2023.120622

Liu, G., Li, S., Song, K., Wang, X., Wen, Z., Kutser, T., Jacinthe, P.-A., Shang, Y., Lyu, L., Fang, C., Yang, Y., Yang, Q., Zhang, B., Cheng, S., Hou, J., 2021. Remote sensing of CDOM and DOC in alpine lakes across the Qinghai-Tibet Plateau using Sentinel-2A imagery data. Journal of Environmental Management 286, 112231. https://doi.org/10.1016/j.jenvman.2021.112231

Liu, H., 2023. Human activity intensity dataset of the Qinghai-Tibet Plateau (2000-2020). National Tibetan Plateau Data Center. https://doi.org/10.3974/geodb.2023.07.08.V1

Liu, L., Yang, S., Wang, S., Hu, J., Li, C., Yi, Y., 2025. Influence of the cascade reservoir operation of the Yellow River on the hydrological regime of the mainstream of the Yellow River. Yellow River 47, 42-47+77.

https://doi.org/10.5194/egusphere-2026-731
Preprint. Discussion started: 19 February 2026

Liu, P., Zeng, H., Qi, L., Degen, A.A., Boone, R.B., Luo, B., Huang, M., Peng, Z., Qi, T., Wang, W., 2024. Vegetation redistribution is predicted to intensify soil organic carbon loss under future climate changes on the Tibetan Plateau. Science of The Total Environment 932, 173034.

Long, J., Wang, L., Chen, D., Li, N., Zhou, J., Li, X., Guo, X., Liu, H., Chai, C., Fan, X., 2024. Hydrological Projections in the Third Pole Using Artificial Intelligence and an Observation‐Constrained Cryosphere‐Hydrology Model. Earth's Future 12, e2023EF004222. https://doi.org/10.1029/2023EF004222

Ma, M., Wang, Z., Zang, H., Wang, W., Wei, M., Cui, H., 2023. Runoff Simulation and Prediction in the Source Region of the Yellow River Based on SSP Scenarios. Journal of North China University of Water Resources and Electric Power (Natural Science Edition) 44, 31–40. https://doi.org/10.19760/j.ncwu.zk.2023054

Ma, W., Wu, T., Wu, X., Yang, S., Li, R., Zhou, S., Li, X., Zhu, X., Hao, J., Ni, J., 2023. Carbon budgets and environmental controls in alpine ecosystems on the Qinghai-Tibet Plateau. Catena 229, 107224.

Maavara, T., Chen, Q., Van Meter, K., Brown, L.E., Zhang, J., Ni, J., Zarfl, C., 2020. River dam impacts on biogeochemical cycling. Nature Reviews Earth & Environment 1, 103–116.

Maavara, T., Lauerwald, R., Regnier, P., Van Cappellen, P., 2017. Global perturbation of organic carbon cycling by river damming. Nature communications 8, 15347.

Meng, Y., Duan, K., Shi, P., Shang, W., Li, S., Cheng, Y., Xing, L., Chen, R., He, J., 2023. Sensitive temperature changes on the Tibetan Plateau in response to global warming. Atmospheric Research 294, 106948.

https://doi.org/10.5194/egusphere-2026-731
Preprint. Discussion started: 19 February 2026

Peng, S., 2025a. 1-km monthly mean temperature dataset for china (1901-2024). National Tibetan Plateau Data Center. https://doi.org/10.11888/Meteoro.tpdc.270961

Peng, S., 2025b. 1-km monthly precipitation dataset for China (1901-2024). National Tibetan Plateau Data Center. https://doi.org/10.5281/zenodo.3114194

Ran, L., Butman, D.E., Battin, T.J., Yang, X., Tian, M., Duvert, C., Hartmann, J., Geeraert, N., Liu, S., 2021. Substantial decrease in CO2 emissions from Chinese inland waters due to global change. Nat Commun 12, 1730. https://doi.org/10.1038/s41467-021-21926-6

San, M., Jia, S., Yang, C., Liu, J., Yu, Z., Fang, W., Shang, J., Ming, B., Guo, Y., Cheng, L., 2025. Runoff Prediction in the Source Region of the Yellow River Basin Based on the CMIP6 Climate Model. Soil and Water Conservation in China 71-77+89. https://doi.org/CNKI:SUN:ZGSB.0.2025-07-020

Vachon, D., Sponseller, R.A., Karlsson, J., 2021. Integrating carbon emission, accumulation and transport in inland waters to understand their role in the global carbon cycle. Global Change Biology 27, 719–727. https://doi.org/10.1111/gcb.15448

Wang, J., Wu, W., Zhou, X., Li, J., 2022. Carbon dioxide (CO2) partial pressure and emission from the river-reservoir system in the upper Yellow River, northwest China. Environ Sci Pollut Res 30, 19410–19426. https://doi.org/10.1007/s11356-022-23489-5

Wang, L., 2024. Difference and causes of runoff in different sections above Tangnaihai in the source region of the Yellow River. Journal of Qinghai Normal University (Natural Science Edition) 40, 99-104+112. https://doi.org/10.16229/j.cnki.issn1001-7542.2024313

Wang, M., Sun, K., Jia, J., Yu, G., Gao, Y., 2026. Unraveling the carbon fraction heterogeneity in China's Rivers: Hydrology, nutrients, and dam regulation. Water Research 288, 124591.

https://doi.org/10.5194/egusphere-2026-731
Preprint. Discussion started: 19 February 2026

https://doi.org/10.1016/j.watres.2025.124591

Wang, S., Benoit, G., Raymond, P.A., Yu, G., Zhou, F., Liu, S., Miao, C., Sun, K., Li, Z., Jia, J., 2025. Dissolved carbon storage and flux dynamics in China's inland waters over the past 30 years. National Science Review nwaf229.

Wang, T., Yang, D., Yang, Y., Piao, S., Li, X., Cheng, G., Fu, B., 2020. Permafrost thawing puts the frozen carbon at risk over the Tibetan Plateau. Science Advances 6, eaaz3513. https://doi.org/10.1126/sciadv.aaz3513

Wang, W., Zhong, J., Li, S.-L., Ulloa-Cedamanos, F., Xu, Sen, Chen, S., Lai, M., Xu, Sheng, 2023. Constraining the sources and cycling of dissolved inorganic carbon in an alpine river, eastern Qinghai-Tibet Plateau. Science of The Total Environment 901, 166262. https://doi.org/10.1016/j.scitotenv.2023.166262

Wang, X., Ma, H., Li, R., Song, Z., Wu, J., 2012. Seasonal fluxes and source variation of organic carbon transported by two major Chinese Rivers: The Yellow River and Changjiang (Yangtze) River. Global Biogeochemical Cycles 26. https://doi.org/10.1029/2011GB004130

Wen, W., Gao, L., Cheng, H., Xiao, L., Zhang, S., Li, S., Jiang, X., Xia, X., 2024. Legacy and alternative perfluoroalkyl acids in the Yellow River on the Qinghai-Tibet Plateau: Levels, spatiotemporal characteristics, and multimedia transport processes. Water Research 262, 122095. https://doi.org/10.1016/j.watres.2024.122095

Wu, Y., Su, H., Cheng, L., Qin, S., Zou, K., Liu, Y., Zhou, J., Liu, P., Zhang, L., 2024. Exploring hydrological controls on dissolved organic carbon export dynamics in a typical flash flood catchment using a process-based model. Science of The Total Environment 921, 171139. https://doi.org/10.1016/j.scitotenv.2024.171139

https://doi.org/10.5194/egusphere-2026-731
Preprint. Discussion started: 19 February 2026

Xu, S., Li, S.-L., Bufe, A., Klaus, M., Zhong, J., Wen, H., Chen, S., Li, L., 2024. Escalating Carbon Export from High-Elevation Rivers in a Warming Climate. Environ. Sci. Technol. 58, 7032–7044. https://doi.org/10.1021/acs.est.3c06777

Yan, N., Qiu, Z., Zhang, C., Liu, J., Liu, D., 2025a. Observing water turbidity in Chinese rivers using Landsat series data over the past 40 years. Journal of Cleaner Production 494, 145001. https://doi.org/10.1016/j.jclepro.2025.145001

Yan, N., Qiu, Z., Zhang, C., Yan, Y., Liu, D., 2025b. Landsat monitoring reveals the history of river organic pollution across China during 1984–2023. Water Research 275, 123210. https://doi.org/10.1016/j.watres.2025.123210

Yan, Y., Lauerwald, R., Wang, X., Regnier, P., Ciais, P., Ran, L., Gao, Y., Huang, L., Zhang, Y., Duan, Z., 2023. Increasing riverine export of dissolved organic carbon from China. Global Change Biology 29, 5014–5032.

Yang, J., Wang, T., Yang, D., Yang, Y., 2023. Insights into runoff changes in the source region of Yellow River under frozen ground degradation. Journal of Hydrology 617, 128892. https://doi.org/10.1016/j.jhydrol.2022.128892

Yang, M., Li, S., Wang, S., Huang, Q., Shen, Q., Kang, Y., Shi, M., Zhang, Y., Luo, D., 2025. Latitudinal gradient and environmental drivers of soil organic carbon in permafrost regions of the Headwater Area of the Yellow River. Carbon Neutrality 4, 16.

Yao, T., Bolch, T., Chen, D., Gao, J., Immerzeel, W., Piao, S., Su, F., Thompson, L., Wada, Y., Wang, L., Wang, T., Wu, G., Xu, B., Yang, W., Zhang, G., Zhao, P., 2022. The imbalance of the Asian water tower. Nat Rev Earth Environ 3, 618–632. https://doi.org/10.1038/s43017-022-00299-4

https://doi.org/10.5194/egusphere-2026-731
Preprint. Discussion started: 19 February 2026

Zeng, F., Song, C., Cao, Z., Xue, K., Lu, S., Chen, T., Liu, K., 2023. Monitoring inland water via Sentinel satellite constellation: A review and perspective. ISPRS Journal of Photogrammetry and Remote Sensing 204, 340–361. https://doi.org/10.1016/j.isprsjprs.2023.09.011

Zhang, X., Liu, H., Xing, Z., 2011. Challenges and Solutions for Sustainable Land Use in Ruoergai-the Highest Altitude Peatland in Qinhai-Tibetan Plateau, China. Energy Procedia 5, 1019–1025. https://doi.org/10.1016/j.egypro.2011.03.180

Zhang, Z., Zhang, L., Liu, Y., Jin, M., 2024. Responses of annual streamflow variability to annual precipitation, extreme climate events and large-scale climate phenomena in the Qinghai-Tibet Plateau. Journal of Hydrology 632, 130969. https://doi.org/10.1016/j.jhydrol.2024.130969

Zhao, W., Cheng, Y., Jian, J., Jiao, J., Cheng, C., Li, J., Chen, T., 2023. Water erosion changes on the Qinghai-Tibet Plateau and its response to climate variability and human activities during 1982–2015. CATENA 229, 107207. https://doi.org/10.1016/j.catena.2023.107207

Zhi, W., Appling, A.P., Golden, H.E., Podgorski, J., Li, L., 2024. Deep learning for water quality. Nat Water 2, 228–241. https://doi.org/10.1038/s44221-024-00202-z